Molecular Dynamic Simulation of Disorder Induced Amorphization in Pyrochlore

A. Chartier,[1,*] C. Meis,[2] J.-P. Crocombette,[3] W. J. Weber,[4] and L. R. Corrales[4]

[1]*CEA-Saclay, DEN/DPC/SCP, Bâtiment 450 Sud, 91191 Gif-Sur-Yvette, France*

[2]*INSTN-Saclay, UEPEM, 91191 Gif-Sur-Yvette, France*

[3]*CEA-Saclay, DEN/DMN/SRMP, Bâtiment 520, 91991 Gif-Sur-Yvette, France*

[4]*Pacific Northwest National Laboratory, P.O. Box 999, Richland, Washington 99352, USA*

(Received 18 August 2004; published 19 January 2005)

The defect accumulation mechanism of amorphization has been studied for the $La_2Zr_2O_7$ pyrochlore by means of classical molecular dynamic simulations. Present calculations show that the accumulation of cation Frenkel pairs is the main driving parameter for the amorphization process, while the oxygen atoms simply rearrange around cations. Under Frenkel pair accumulation, the structure follows the pyrochlore-fluorite-amorphous sequence. Present results consequently provide atomic-level interpretation to previous experimental irradiation observations of the two-step phase transition.

DOI: 10.1103/PhysRevLett.94.025505 PACS numbers: 61.43.Bn, 61.72.Ji, 81.30.–t

Radiation-induced amorphization has a significant impact on the long-term durability of pyrochlores proposed for immobilization of nuclear waste [1]. Despite the great number of experimental and theoretical studies that have been devoted to understanding radiation-induced amorphization in pyrochlores, the amorphization mechanisms remain unresolved.

Rare earth zirconates pyrochlores $A_2Zr_2O_7$, where $A =$ Gd, Er, Nd, or Sm, exhibit an extremely high radiation resistance [2–4] even at low temperatures (~ 25 K), remaining crystalline up to doses of 7.0 dpa (displacements per atom). $La_2Zr_2O_7$ becomes amorphous at temperatures lower than 310 K [4] for doses of roughly 1–2 dpa when irradiated by 1.5 MeV Xe^+. According to studies by Lian *et al.* [4,5], $La_2Zr_2O_7$ under irradiation first goes through a disordering of the oxygen sublattice with a random occupation of the structural oxygen vacancy. Continued irradiation leads to a transition to the disordered fluorite phase where both cations and anions are randomly distributed (see Hess *et al.* [6]). Eventually, amorphization takes place. In this theoretical study, without dealing explicitly with the difference between the behavior of the La zirconate and the other pyrochlores under irradiation, we provide evidence that the cation Frenkel pair accumulation is the principal mechanism through which the pyrochlore structure may transit to the fluorite state and eventually to the amorphous one, as observed by Lian *et al.*

In fact, previous numerical studies [7] have shown that point defect accumulation in $La_2Zr_2O_7$ plays a major role in the amorphization process. Single event displacement cascades in lanthanum zirconate pyrochlore at 350 K, induced by a uranium primary knock-on atom (pka) accelerated at 6 keV, produce only point defects. Those simulations have revealed that 90% of the displaced atoms recombine almost instantaneously. Most of the point defects created are oxygen Frenkel pairs (FPs), while 67% of the defective cations are found in antisites (ASs), and only 33% of them occupy interstitial positions. The cation FP formation energies of 6 and 14 eV for La and Zr, respectively, as well as the cation AS formation energy, roughly 2 eV, are also reflected in the cascades final state.

Limoge *et al.* [8] first studied amorphization by accumulation of point defects with molecular dynamic (MD) simulations in a pure Lennard-Jones crystal, which showed that amorphization is triggered above the critical concentration and introduction rate of point defects. Subsequent molecular dynamics studies of the effect of point defect accumulation in binary alloys or semiconductors (see, for example, Ref. [9]) have shown that the number of introduced Frenkel pairs is the driving parameter for the disordered induced amorphization process.

Here in this work an analogous method is used for ceramic oxides to investigate the amorphization transition due to defect accumulation. We introduce different concentrations of point defects (ASs or FPs) in $La_2Zr_2O_7$ as the initial states of MD simulations to determine the critical defect concentration beyond which the matrix transits to another crystalline state and/or collapses to an amorphous state.

$La_2Zr_2O_7$ pyrochlore is an ordered form of the cubic fluoritelike arrangement of atoms. Cations build a fcc network, with La and Zr lying along the opposite diagonals of the faces of the cube. The oxygen sublattice is cubic with an intrinsic vacancy surrounded by Zr atoms, in such a way that LaO_8 and ZrO_6 polyhedrons are formed. Conversely, in the disordered fluorite structure, cations as well as anions are randomly distributed in their sublattices. This leads, on average, to LaO_7 and ZrO_7 polyhedrons and to an occupation of 7/8th of the oxygen sites. As a by-product, the body-centered site of the fcc cation sublattice, which is also the only interstitial site, becomes another equivalent origin with respect to which all cations can be translated, without any modification of the structure.

A cell containing 704 atoms is used where the atomic interactions are purely ionic and described by Coulomb interactions complemented by short-range Buckingham

potentials for cation-oxygen pairs. The set of parameters of these potential interactions has been fitted on experimental and *ab initio* data for the ordered pyrochlore $La_2Zr_2O_7$ using the GULP code [10]. Extensive details are given in Ref. [7]. Various disordered fluorite and amorphous states were generated using the same set of parameters.

The computational generation of the disordered fluorite phase was done by a random inversion of half the cations of each type resulting in AS configurations. No oxygen atom disorder was introduced. During an MD run of 18 ps the oxygen atoms spontaneously moved such that a disordered fluorite structure was obtained, as evidenced by the radial distribution functions (RDFs) as well as by the appearance of LaO_7 and ZrO_7 polyhedrons.

In the transition from the pyrochlore to the fluorite structure, the calculated average Gibbs free energy at 300 K, obtained from the phonon density of states of the quenched phases, as implemented in the GULP code [10], is increased by 0.092 eV/atom. This is comparable to the 0.096 eV/atom free energy change measured for the order to disorder transition in $MgAl_2O_4$ [11]. The calculated average bulk modulus is slightly lowered by 3.6% compared to the one of pyrochlore, in agreement with what is observed experimentally in gadolinium zirconate [12]. The calculated mean volume is also lowered by 1.3%, which is in contradiction with the experimental observation of +0.1% in gadolinium zirconate [6]. It is worth noting that some oxides, e.g., spinels [13], show either swelling or shrinkage upon disordering depending on their composition.

The amorphous state was obtained by quenching the perfect pyrochlore from 6000 towards 300 K, with a linear cooling rate of 30 K/ps. The analysis of the partial RDF of the final state shows that M-O distances (M being La or Zr) are reduced by 10%, which is roughly in the range of the 7% decrease observed in natural pyrochlore samples by Lumpkin [14]. The O-O partial RDF is mainly flat above the 4 Å peak, in good agreement with experiment [14–16]. Present calculations show a swelling of 8.3%, also in close agreement with experimental observations of between 5% and 10%, depending on the accumulation dose received in gadolinium titanate [17]. The calculated Gibbs free energy difference between the crystalline pyrochlore and the amorphous states at 300 K is 0.35 eV/atom.

According to the results presented above, the parameter set of this empirical potential does an excellent job describing the perfect pyrochlore structure, as well as the fluorite and the amorphous structures.

Throughout this study, the FP or AS defects are introduced in a *randomly* distributed manner in the simulation cell. The cell is then thermalized at 300 K, at constant volume, or at constant pressure by rescaling the velocities of the atoms during 4 ps. This prevents the atoms from being artificially accelerated when subjected to strong repulsive potentials resulting from the introduction of interstitials. Thus, the system is forced to stabilize in a metastable configuration. An MD run of 18 ps is then performed. The final structure is analyzed in terms of atomic configurations and internal energy.

To distinguish pyrochlore and disordered fluorite, simple tests on the number and nature of oxygen vacancies and cations neighbors were applied. Disorder on the oxygen sublattice is calculated by counting the occupation number of the oxygen sublattice. For the disordered fluorite state, this number should be 7/8th for all the oxygen sites, whereas it is zero for the intrinsic vacancy and one for the occupied oxygen sites, in pyrochlore. To calculate the disorder on the cation sublattice, the type of second neighbors of cations (at 5.4 Å) must be considered. In pyrochlore the second neighbor cations are entirely heteroatomic, while in disordered fluorite half are homoatomic and half are heteroatomic. Those criteria are translated as order parameters (OPs), such that

$$\mathrm{OP}(n) = \frac{|n - n(\mathrm{fluo})|}{|n(\mathrm{fluo}) - n(\mathrm{pyro})|},$$

where n is the number of neighbors (vacancies) for cations (anions). Thus, for OP = 0, the structure is fluorite. Cation interstitials are evidenced by the occurrence of 2.7 Å cation-cation distances. Some systems exhibit amorphous states, which are identified by their partial RDFs and energy equivalent to the ones of the thermal amorphous reference state.

We first explore the transition of the pyrochlore structure towards the disordered fluorite by introducing antisites. For that purpose, 140 configurations have been randomly generated, sampling the number of ASs from 0%, the perfect pyrochlore structure, to 100% corresponding to the disordered fluorite structure. For all configurations, no cation FPs appear during the simulation and the resulting structures show only cation ASs. As before, oxygen disorder was not introduced; however, the oxygens spontaneously moved during the MD run so that cation first shell is reorganized (as expected from static calculations [7]). The disorder that appears on the oxygen sublattice follows almost perfectly the disorder introduced for cations, as can be seen in Fig. 1. Oxygen atoms positions are consequently driven by cations. This is consistent with the suggestion by Hess *et al.* [6] that, in gadolinium pyrochlores, the pyrochlore to fluorite transition is mainly driven by cations.

In a second step, in order to have a view of the early stage of radiation damage in perfect pyrochlore, different concentrations of randomly generated Frenkel pairs, up to 16% of the cations were introduced. To reproduce the ratio of the remaining point defects observed in displacements cascades [7], twice as many lanthanum as zirconium FPs were introduced. In both cases, no amorphization is observed up to 16% of Frenkel pairs, but the cells gradually transit towards the disordered fluorite structure, as can be seen on the increase in AS population (Fig. 2). The FP per

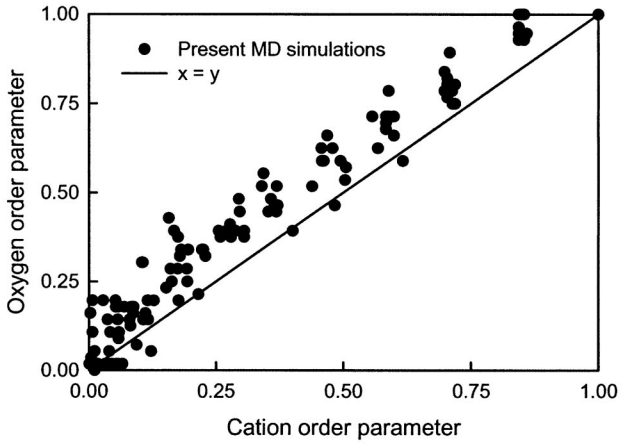

FIG. 1. Oxygen versus cations order parameters [(OPs); see equation in the text] for the introduction of antisites in perfect pyrochlore at constant volume. Oxygen OP is almost equal to cation OP.

cation ratio required to fully transform the pyrochlore to the fluorite structure can be estimated to be around 0.2.

The number of remaining FPs at the end of the *NPT* runs show an apparently anomalous behavior. At concentrations less than 7.8%, as more FPs are introduced, fewer FPs remain at the end of the simulations. At concentrations larger than 7.8%, no FPs remain at the end of the simulation. This can be explained by considering that, for large initial concentrations, the interstitial-vacancy pairs are unstable as their distances are smaller than the recombination radius. From this, it can be deduced that the recombination radius is about 8 Å, which corresponds to the third neighbor cation-cation distance. In contrast, for *NVT* runs, all FPs recombine regardless of their initial concentration. This implies that the FP recombination radius is larger than the size of the present cell in *NVT*. That can be explained by the very large stress induced by the FPs, whereas ASs do not create any stress (compare the swellings of the fluorite and amorphous states). Thus, we show that, under the introduction of FPs, perfect pyrochlore transits first to the fluorite structure. In view of what happens under irradiation, this provides atomic-level interpretation of the experimental observations by Lian *et al.* [4,5] for $La_2Zr_2O_7$.

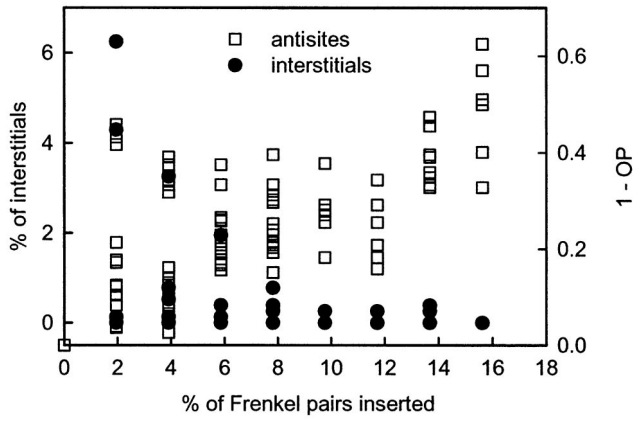

FIG. 2. Remaining defects (after *NPT* simulations) as a function of the percentage of Frenkel pairs inserted in the perfect pyrochlore. OP sets for order parameter.

To model the further evolution of pyrochlore under irradiation, Frenkel pairs in the disordered fluorite structure were introduced. At constant volume, no matter the amount of FPs, no transition to the amorphous state is observed, although a slight increase in energy occurs, which readily reaches a maximum (see Fig. 3). At constant pressure, the introduction of more than 10% FPs (with the same ratio between La and Zr FPs) does lead to a transition to the amorphous state. Lower initial concentrations of FPs do not trigger the amorphization process.

In view of these results, we can draw a complete picture of the processes taking place in zirconate pyrochlores under irradiation. The oxygen atoms play little role in the order-disorder transitions because the cation order parameter drives that of the oxygen atoms. Accumulation of FPs is the mechanism that drives zirconium pyrochlores towards amorphization following a two-step process: First, a transition from pyrochlore to disordered fluorite that occurs for about a 0.2 FP per cation ratio in $La_2Zr_2O_7$. Second, subsequent irradiation produces more FPs, and the amorphization of disordered fluorite $La_2Zr_2O_7$ takes place for a critical FP concentration of 0.1. In the low temperature limit a total number of $0.2 \pm 0.1 = 0.3$ FPs per cation should be produce by irradiation to fully amorphize lanthanum zirconate pyrochlore.

The amorphization thus relies on the ability to reach a significantly high critical FP concentration before the crystalline structure collapses. This mechanism provides

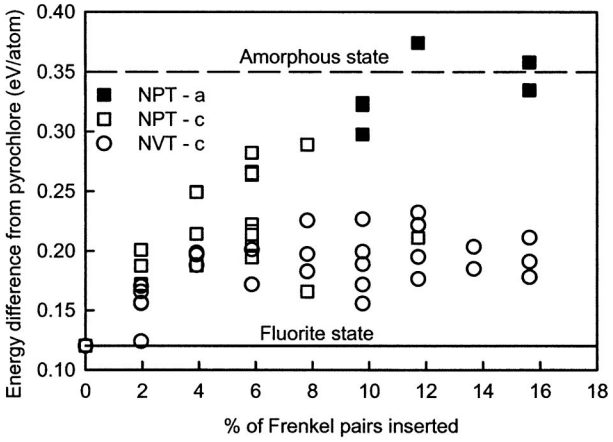

FIG. 3. Energy differences (eV/atom) between the resulting states and the perfect pyrochlore as a function of the FP inserted in the fluorite structure, at constant pressure (*NPT*, squares) and constant volume (*NVT*, circles). Solid (open) symbols denote amorphous (a) [crystalline (c)] states. Energies of the reference states are represented by lines.

atomic-level interpretation of the difficulty to amorphize lanthanum zirconate, as evidenced by its low critical temperature of 310 K [4,5]. As soon as the temperature is large enough to activate the diffusion of cation vacancies or interstitials, recombination takes place, and it becomes impossible to reach the critical concentration. Such diffusive recombination processes may prevent the amorphization of the other zirconate pyrochlores.

This research was supported in part by the Office of Basic Energy Sciences, U.S. Department of Energy under Contract No. DE-AC06-76RL 1830.

*Electronic address: achartier@CARNAC.CEA.FR

[1] R. C. Ewing, W. J. Weber, and J. Lian, J. Appl. Phys. **95**, 5949 (2004).
[2] S. X. Wang, B. D. Begg, L. M. Wang, R. C. Ewing, W. J. Weber, and K. V. Govidan Kutty, J. Mater. Res. **14**, 4470 (1999).
[3] K. E. Sickafus, L. Minervini, R. W. Grimes, J. A. Valdez, M. Ishimaru, F. Li, K. J. McClellan, and T. Hartmann, Science **289**, 748 (2000).
[4] J. Lian, X. T. Zu, K. V. Govidan Kutty, J. Chen, L. M. Wang, and R. C. Ewing, Phys. Rev. B **66**, 54 108 (2002).
[5] J. Lian, L. Wang, J. Chen, K. Sun, R. C. Ewing, J. Matt Farmer, and L. A. Boatner, Acta Mater. **51**, 1493 (2003).
[6] N. J. Hess, B. D. Begg, S. D. Conradson, D. E. McCready, P. L. Gassman, and W. J. Weber, J. Phys. Chem. B **106**, 4663 (2002).
[7] A. Chartier, C. Meis, J.-P. Crocombette, L. R. Corrales, and W. J. Weber, Phys. Rev. B **67**, 174102 (2003).
[8] Y. Limoge, A. Rahman, H. Hsieh, and S. Yip, J. Non-Cryst. Solids **99**, 75 (1988).
[9] M. J. Sabochick and N. Q. Lam, Phys. Rev. B **43**, 5243 (1991); H. Hsieh and S. Yip, Phys. Rev. B **39**, 7476 (1989); R. Devanathan, F. Gao, and W. J. Weber, Appl. Phys. Lett. **84**, 3909 (2004).
[10] J. D. Gale and A. L. Rohl, Mol. Simul. **29**, 291 (2003).
[11] E. Stoll, J. Phys. (France) **25**, 447 (1964).
[12] M. P. Van Dijk, K. J. de Vries, and A. J. Burggraaf, Solid State Ionics **9&10**, 913 (1983).
[13] R. M. Hazen and H. Yang, Am. Mineral. **84**, 1956 (1999).
[14] G. R. Lumpkin, J. Nucl. Mater. **289**, 136 (2001).
[15] R. B. Greegor, F. W. Lytle, B. C. Chakoumakos, G. R. Lumpkin, J. K. Warner, and R. C. Ewing, in *Proceedings of the Scientific Basis for Nuclear Waste Management XII*, edited by W. Lutze and R. C. Ewing (Materials Research Society, Warrendale, PA, 1989), Vol. 127, p. 261.
[16] G. K. Krivokoneva and G. A. Sidorenko, Geochem. Int. **8**, 113 (1971).
[17] W. J. Weber, J. W. Wald, and Hj Marzke, Mater. Lett. **2**, 173 (1985).